Enhancing Remedial Performance Assessments at a Complex Site Using CSIA and Molecular Biological Tools

Dr. Julie Konzuk (jkonzuk@geosyntec.com), Carol Cheyne, Dr. Lisa D'Agostino, and Dr. Michelle Cho - Geosyntec Consultants, Dr. Bryan Goodwin – Goodwin Remediation Consulting Pty Ltd, and Camillo Coladonato – Dow Chemical (Australia) Pty Ltd

ABSTRACT

Delta carbon-13 ($\delta^{13}C$) compound-specific isotope analysis (CSIA) and molecular biological tools (MBTs) datasets were analyzed to support evaluation of enhanced in situ bioremediation (EISB) and monitored natural attenuation (MNA) performance in attenuating chlorinated volatile organic compounds (CVOCs) at a complex fractured basalt site. The objectives of the analysis was to evaluate the extent of degradation, identify potential/likely degradation mechanisms, estimate degradation rates and assess temporal and spatial changes in degradation activity in both the source zones and downgradient areas where MNA dominated.

Site-specific enrichment factors (ε) were estimated based on temporal changes in $\delta^{13}C$ signatures using Modified Kuder plots at individual locations for seven CVOCs. As a quality assurance step, the estimated ε were compared to literature values. MBT data were also compared to the dominant degradation mechanisms interpreted from ε values as an additional line of evidence to support the interpreted degradation mechanisms. The ε values were then used to estimate first-order degradation rates and associated half-lives.

Estimated ε values supported dominance of anaerobic biodegradation pathways for PCE, TCE, 1,1,2-TCA, CF, and EDC in active EISB zones. VC appears to be degrading under both aerobic biodegradation and abiotic degradation pathways near a zero-valent iron permeable reactive barrier. Outside of EISB zones, there is evidence for aerobic (co)metabolic degradation of EDC. Consistently increasing enrichment in the $\delta^{13}C$ signatures of the primary DNAPL components 1,1,2-TCA and EDC confirms that EISB is reducing source mass. $\delta^{13}C$ signatures in the plumes downgradient of the EISB area confirm limited natural biological attenuation is ongoing, with the exception of VC, which biodegrades aerobically. Calculated half-lives were typically shorter in the bioactive zone and longer in the downgradient area, consistent with enhanced bioactivity in the EISB area and MNA downgradient.

Background/Objectives

Enhanced in situ bioremediation (EISB) using a soluble partitioning donor (propylene glycol) has been in progress for over a decade at a complex site containing multiple dense, non-aqueous phase liquid (DNAPL) sources in fractured basalt bedrock. During this time period, a comprehensive dataset of chlorinated volatile organic compound (CVOC) concentrations, various biogeochemical parameters, delta carbon-13 ($\delta^{13}C$) compound-specific isotopic analysis (CSIA), and quantitative polymerase chain reaction (qPCR) microbial data was collected. This dataset included multiple timepoints at multiple locations both within the EISB treatment zone, as well as downgradient locations where monitored natural attenuation (MNA) was ongoing. Over the years of monitoring, the dataset was qualitatively reviewed to confirm that biodegradation was ongoing (e.g. indications of $\delta^{13}C$ enrichment and/or elevated qPCR concentrations combined with CVOC concentration reductions). Quantification of biodegradation rates for various CVOCs using the CSIA data had not yet been attempted.

Given the complexity of the site conditions, there was a desire to better quantify biodegradation rates and evaluate the extent of degradation of source mass. These complexities include multiple DNAPL sources with different source compositions, primary and secondary porosities in the bedrock with the potential for back-diffusion sources, and potentially inhibitory levels of chloroform (CF) in multiple areas that could slow down activity of certain microbes. Additionally, the comprehensive dataset, encompassing a range of CVOC concentrations, $\delta^{13}C$ values, and variable microbial signatures, provided a unique opportunity to gain insight into site-specific attenuation behavior and factors influencing this behavior.

The objective of this work was to develop a workflow and process for estimating site-specific enrichment factors, and use those, combined with the $\delta^{13}C$, qPCR and biogeochemical data, to evaluate the extent of degradation, identify potential degradation mechanisms, estimate degradation rates, and better understand remedy performance for attenuating CVOCs in both the source areas and downgradient plumes.

TABLE 1: Chosen $\delta^{13}C$ source signatures compared to those reported in the literature..

CVOC	Literature-Reported $\delta^{13}C_o$ (‰) [3]	Source / Plume 1 $\delta^{13}C_o$ (‰)	Source / Plume 2 $\delta^{13}C_o$ (‰)
1,1,2,2-TeCA	-40.1 ≤ -39.7 ≤ -39.2	-41.6 [1]	-48.0 [1]
1,1,2-TCA	-36.0	-38.8 [1]	-50.7 [1]
1,2-DCA	-31.0 ≤ -29.2 ≤ -27.3	-25.2 [2]	-38.2 [1]
PCE	-37.4 ≤ -29.1 ≤ -23.2	-40.7 [2]	-40.7 [2]
TCE	-35.6 ≤ -29.3 ≤ -23.0	-54.0 [1]	-54.5 [1]
VC	-29 ≤ -28 ≤ -27	-48.5 [1]	-58.6 [1]
CF	-63.6 ≤ -50.9 ≤ -43.2	-41.5 [1]	-52.5 [1]

[1] Average of three most-negative groundwater $\delta^{13}C$ values.
[2] Average DNAPL $\delta^{13}C$ signature.
[3] Shown as Minimum ≤ Average ≤ Maximum

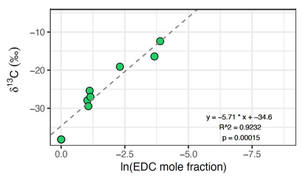

FIGURE 1: Example Modified Kuder plot illustrating the range in $\delta^{13}C$ signatures measured at a specific location over time and the corresponding best-fit model, where the slope corresponds to the enrichment factor (i.e. ε = -5.71 permil [‰]).

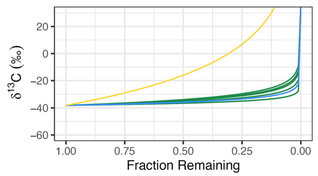

FIGURE 2: Rayleigh models plotted using the minimum (blue line) and maximum (yellow line) literature-reported enrichment factors compared to the best-fit enrichment factors at a number of locations (green lines) for 1,2-DCA. In this example, the best-fit ε match well with the minimum-reported literature values.

Approach

$\delta^{13}C$ data for groundwater and DNAPL samples collected from >50 wells over a decade were used to estimate best-fit site-specific ε for seven CVOCs (including 1,1,2,2-tetrachloroethane [1,1,2,2-TeCA], 1,1,2-trichloroethane [1,1,2-TCA], 1,2-dichloroethane [1,2-DCA], vinyl chloride [VC], tetrachloroethene [PCE], trichloroethene [TCE], and chloroform [CF]). Of these, 1,1,2,2-TeCA, 1,1,2-TCA, 1,2-DCA and PCE represented DNAPL constituents. 1,2-DCA, TCE, VC and CF were all daughter products, sometimes of multiple degradation pathways (e.g. generation of VC from degradation of 1,1,2-TCA, 1,2-DCA, or cis-1,2-dichloroethene).

Source $\delta^{13}C$ signatures (**Table 1**) were chosen either from DNAPL $\delta^{13}C$ signatures (1,2-DCA where the DNAPL was primarily 1,2-DCA, and PCE), or as the average of three most-negative groundwater $\delta^{13}C$ signatures (1,1,2,2-TeCA, 1,1,2-TCA, 1,2-DCA where it was a minor component of the DNAPL source, TCE, VCM, and CF). Of note, the $\delta^{13}C$ signatures of 1,1,2,2-TeCA and 1,1,2-TCA in a stored DNAPL sample were observed to become more positive when re-analyzed three years later, likely due to ongoing dehydrochlorination of 1,1,2,2-TeCA (~1.0-year half-life at 15 degrees celcius) and anaerobic dichloroelimination of 1,1,2-TCA.

TABLE 2: Best-fit site-specific ε factors and comparable values reported in the literature.

CVOC	Best-Fit Site-Specific ε (‰) [1]	Literature-Reported ε (‰) [2,3]	Literature-Reported Degradation Mechanisms [4]
1,1,2,2-TeCA	-4.2 ± 0.8‰	-25.6 to -27.1	Dehydrochlorination (abiotic)
		-12.7 to -19.3	Dichloroelimination (abiotic)
1,1,2-TCA	-7.0 ± 1.3‰	-0.72 ± 0.12	Anaerobic biodegradation (*Dsb* and *Dhc*)
		-6.9 ± 0.4	Anaerobic biodegradation (*Dhg*)
		-2.0 ± 0.2	Anoxic microcosms (uncharacterized)
		-14.6 ± 0.7	Abiotic reductive dechlorination
1,2-DCA	-4.8 ± 0.6‰	-28.4 to -30.9	Anaerobic biodegradation (*Dhc*)
		-23.0 ± 2.0	Anaerobic biodegradation (*Dhg*)
		-7.3 to -16.7	Anaerobic biodegradation (Dihaloelimination)
		-29.0 to -33.0	Anaerobic biodegradation (*Dhc*)
		-32 ± 1	Anoxic microcosms (uncharacterized)
		-3.5 to -3.9	Aerobic biodegradation (*Pseudomonas*)
		-25.8 to -31.9	Aerobic/anaerobic biodegradation (hydrolytic dehalogenation)
PCE	-2.0 ± 0.5‰	-6.0	Anaerobic reductive dechlorination (*Dhc*)
		-1.6 ± 0.1	Anaerobic reductive dechlorination (*Geobacter*)
		-30.2 ± 4.3	Abiotic degradation (iron sulfide)
		-5.7	Abiotic degradation (zero-valent iron)
		-17	Abiotic degradation (zero-valent iron)
TCE	-4.9 ± 0.6‰	-2.5 to -22.9	Anaerobic biodegradation
		-1.1 to -11.5	Aerobic biodegradation
		-10.1 to -26.5	Abiotic degradation (zero-valent iron)
VC	-4.9 ± 1.1‰	-3.2 to -8.2	Aerobic biodegradation
	-15.1 ± 2.3‰	-6.9 to -19.4	Abiotic degradation (zero-valent iron)
	-34.5 ± 5.9‰	-21.5 to -28.1	Anaerobic biodegradation
CF	-4.9 ± 0.6‰	-4.3 to -27.5	Anaerobic biodegradation (*Dehalobacter*)
		-29.4 to -33.0	Abiotic degradation (zero-valent iron)

[1] Shown as average ± 95% confidence interval. Three distinct clusters of ε were observed for VC, corresponding to three distinct degradation pathways.
[2] Shown either as a range of values reports (X to X) or as the average ± 95% confidence interval.
[3] References can be provided upon request.
[4] *Dhc* = Dehalococcoides, *Dsb* = Desulfitobacterium, *Dhg* = Dehalogenimonas

Enrichment factors were derived by fitting best-fit lines to Modified Kuder plots (see **Figures 1 and 2** for examples). To be considered a good fit, best-fit lines needed to have a minimum of 4 data points, an R^2 value > 0.5, p-value < 0.1 and a spread > 10%. Best-fit ε were compared to literature-derived ε (**Table 2**) to identify dominant degradation mechanisms. MBT data were compared to the interpreted dominant degradation mechanisms based on ε as evidence to support the interpreted degradation mechanisms. Further, the site-specific ε were used to estimate first-order degradation rates across the site (see example in **Figure 3**), and associated half-lives for CVOCs.

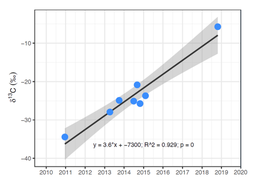

FIGURE 3: Example best-fit curve for 1,2-DCA where the first-order degradation rate *k* = slope of the curve / best-fit ε, and the half-life = ln(0.5) / *-k*.

Conclusions

Best-fit site-specific ε factors supported dominance of anaerobic biodegradation pathways for PCE, TCE, 1,1,2-TCA, CF and EDC in the EISB treatment areas where electron donor persists. VC appears to be degrading under both aerobic biodegradation and abiotic degradation pathways near a zero-valent iron permeable reactive barrier. Consistently increasing enrichment in the $\delta^{13}C$ signatures of the primary DNAPL components 1,1,2-TCA and EDC confirms that ongoing source treatment is reducing source mass.

Outside of the EISB treatment zone, there is some evidence for aerobic (co)metabolic degradation of EDC in the downgradient natural attenuation area. $\delta^{13}C$ signatures in the plumes downgradient of the EISB area confirm that limited natural biological attenuation is ongoing, with the exception of VC, which is biodegrading aerobically.

Calculated half-lives were typically shorter in the bioactive zone and longer in the downgradient area (**Table 3**), consistent with enhancement of bioactivity in the EISB area and natural attenuation downgradient. Several calculated half-lives were less than two years, most often for locations within the EISB treatment zone and downgradient of the source areas where concentrations are typically lower.

TABLE 3: Best-fit degradation half-lives in the EISB treatment zones versus MNA zone.

CVOC	Half-Life in Bioactive Zone (yr)		Half-Life in MNA Zone (yr)	
	High [CF]	Low [CF]	High [CF]	Low [CF]
1,1,2,2-TeCA	--	5.1 (1)	--	--
1,1,2-TCA	1.1 to 3.3 (5)	1.3 to 2.3 (2)	--	4.8 (1)
1,2-DCA	1.2 to 7.3 (7)	2.7 to 4.4 (2)	27 (1)	--
TCE	1.2 to 3.3 (2)	1.3 to 1.9 (3)	0.9 to 6.3 (2)	7.1 (1)
VC	2.5 to 17.4 (2)	--	8.4 (1)	--

[1] The number of calculable half-lives that fit each category is shown in (brackets).
[2] No half-lives could be calculated for PCE or CF.

The results of the isotopic assessment are being used to streamline future sampling events, targeting key locations to monitor EISB performance and changes in offsite degradation activity, coupled with microbial analysis at select locations to gain further insight into dominant degradation mechanisms.

LESSONS LEARNED

Derivation of site-specific ε using Modified Kuder plots of temporal data collected at individual locations/depths was found to provide estimates of ε consistent with reported literature values and consistent with observed microbial activity and/or abiotic degradation related to the presence of zero-valent iron. Ground-truthing the estimated ε values was an important step in the process, however, as the choice of source $\delta^{13}C$ signatures sometimes dictated the estimated ε value. Selection of an appropriate source $\delta^{13}C$ signature was more challenging for compounds that were both present as DNAPL as well as a daughter product of degradation of another compound (e.g. EDC), both of which could have distinctly different source signatures. In addition, estimated ε values should be consistent with reported literature values based on dominant microbial activity (where available).

First-order degradation rates derived from CSIA signatures were also found to be consistent with rates estimated from concentration trends, supporting biological attenuation as the dominant attenuation mechanism for this site.